

# Design and Synthesis of Potent and Selective Macrocyclic Thrombin Inhibitors

Philippe G. Nantermet,<sup>a,\*</sup> James C. Barrow,<sup>a</sup> Christina L. Newton,<sup>a</sup> Janetta M. Pellicore,<sup>a</sup> MaryBeth Young,<sup>a</sup> S. Dale Lewis,<sup>b</sup> Bobby J. Lucas,<sup>b</sup> Julie A. Krueger,<sup>b</sup> Daniel R. McMasters,<sup>c</sup> Youwei Yan,<sup>d</sup> Lawrence C. Kuo,<sup>d</sup> Joseph P. Vacca<sup>a</sup> and Harold G. Selnick<sup>a</sup>

<sup>a</sup>Department of Medicinal Chemistry, Merck Research Laboratories, West Point, PA 19486, USA

<sup>b</sup>Department of Biological Chemistry, Merck Research Laboratories, West Point, PA 19486, USA

<sup>c</sup>Department of Molecular Systems, Merck Research Laboratories, West Point, PA 19486, USA

<sup>d</sup>Department of Structural Biology, Merck Research Laboratories, West Point, PA 19486, USA

Received 12 March 2003; accepted 28 April 2003

This manuscript is dedicated to the memory of our colleague and friend Christie Newton

**Abstract**—A series of potent and selective proline- and pyrazinone-based macrocyclic thrombin inhibitors is described. Detailed SAR studies led to the incorporation of specific functional groups in the tether that enhanced functional activity against thrombin and provided exquisite selectivity against trypsin and tPA. X-ray crystallography and molecular modeling studies revealed the inhibitor-enzyme interactions responsible for this selectivity.

© 2003 Elsevier Ltd. All rights reserved.

Thrombosis-related disorders such as deep vein thrombosis, pulmonary embolism and thromboembolic stroke remain a major cause of morbidity worldwide.<sup>1</sup> The limitations associated with the current therapies<sup>2</sup> have driven the recent search for small-molecule direct inhibitors of specific enzymes involved in the coagulation cascade.<sup>3</sup> Inhibitors of both thrombin and Factor Xa have attracted considerable attention.<sup>4</sup> The search for orally bioavailable direct inhibitors of thrombin has led our laboratories to the evaluation of proline<sup>5</sup> and pyrazinone<sup>6</sup> based small molecules which inhibit thrombin with a high degree of potency and selectivity. In this letter we report on the elaboration of such inhibitors into highly potent and selective macrocycles.

Earlier studies with proline-based inhibitors<sup>5</sup> have shown that a significant enhancement in inhibitory potency is obtained by accessing the S<sub>4</sub> shelf of the enzyme from either the P<sub>1</sub> or P<sub>3</sub> group<sup>7</sup> (Fig. 1). Substitution of the N-terminal amino group (P<sub>3</sub>) with either

*N,N*-diethylacetamide or benzenesulfonamide (**2**, **5**) provided a 10- to 15-fold enhancement in potency while substitution of the P<sub>1</sub> phenol with *N*-ethylacetamide (**3**) resulted in a comparable 8-fold boost in potency. Examination of X-ray crystallographic data<sup>5</sup> revealed the close spatial proximity of lipophilic P<sub>4</sub> groups attached to either P<sub>1</sub> or P<sub>3</sub>. This analysis, along with the

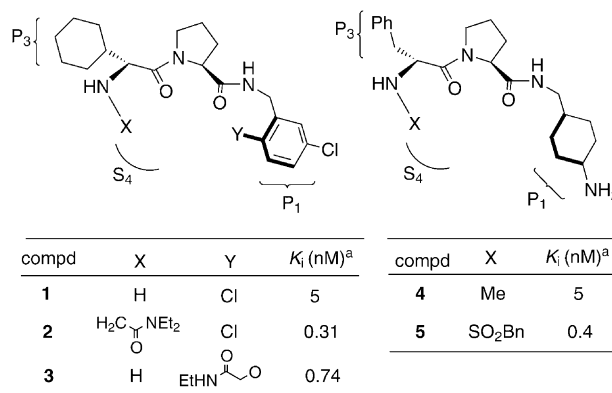


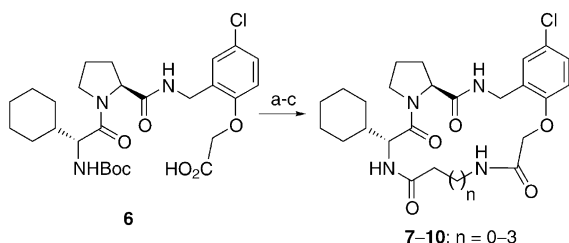
**Figure 1.** <sup>a</sup>K<sub>i</sub> values are the average of at least two determinations, standard error of the mean < 10%.

\*Corresponding author. Tel.: +1-215-652-0945; fax: +1-215-652-3971; e-mail: philippe\_nantermet@merck.com

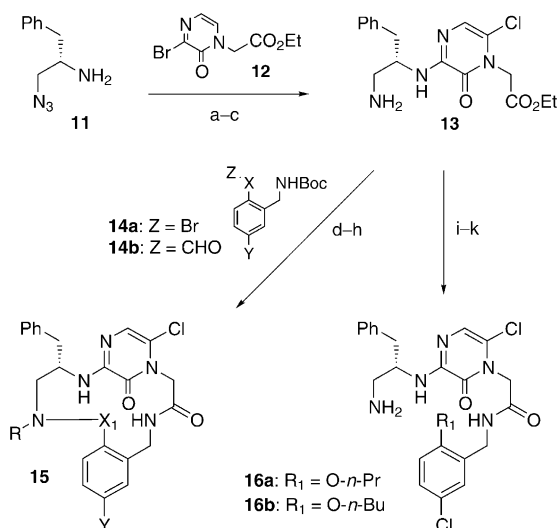
possibility of enhancing potency by conformational preorganization directed us toward the design of macrocycles<sup>8</sup> which would link the P<sub>1</sub> and P<sub>3</sub> groups of a proline-based inhibitor. Ultimately, extension of this concept to pyrazinone-based inhibitors was found to be more fruitful.

The synthesis of proline-derived macrocycles is illustrated in Scheme 1. Coupling of various aminoesters to carboxylic acid **6**<sup>5a</sup> followed by deprotection and macrolactamization provided macrocycles **7–10**.

The preparation of pyrazinone-based macrocycles followed a similar route. Aminoester **13** was prepared from azide **11**<sup>9</sup> and bromopyrazinone **12**<sup>6</sup> according to Scheme 2. Alkylation with bromides **14a** or reductive amination with aldehydes **14b**, followed by deprotection and macrolactamization led to compounds **17–23** and **27–31** of general structure **15**. An alternative macrocyclization strategy<sup>10</sup> based on Grubbs olefin metathesis<sup>11</sup> was implemented for the synthesis of compounds **24–26**. Acyclic inhibitors **16a,b** were prepared from **12** by standard protecting group manipulations and amide coupling.



Scheme 1. (a)  $t\text{BuO}_2\text{C}(\text{CH}_2)_n\text{NH}_2$ , EDC, HOAt, DMF; (b) TFA; (c) EDC, HOAt, DMF.



Scheme 2. (a)  $\text{Et}_3\text{N}$ ,  $110^\circ\text{C}$ ; (b)  $\text{NCS}$ ,  $\text{DCE}$ ,  $80^\circ\text{C}$ ; (c)  $\text{SnCl}_2$ ,  $\text{MeOH}$ ; (d) **14a**,  $\text{Et}_3\text{N}$ ,  $\text{DMF}$  or **14b**,  $\text{NaBH}(\text{OAc})_3$ ,  $\text{DCE}$ ; (e)  $\text{HCl}(\text{g})$ ,  $\text{DCM}$ ; (f)  $1\text{ N LiOH}$ ,  $\text{THF}$ ; (g) EDC, HOAt,  $\text{Et}_3\text{N}$ ,  $\text{DMF}$ ,  $50^\circ\text{C}$ ; (h) for  $\text{R} = \text{Me}$ ,  $\text{HCHO}$ ,  $\text{NaBH}(\text{OAc})_3$ ; (i)  $\text{Boc}_2\text{O}$ ,  $\text{CH}_2\text{Cl}_2$ ; (j)  $1\text{ N LiOH}$ ,  $\text{THF}$ ; (k) 1-(5-chloro-2-propoxyphenyl)methanamine, EDC, HOAt,  $\text{Et}_3\text{N}$ ,  $\text{DMF}$ , microwave  $80^\circ\text{C}$ , 10 min, then  $\text{HCl}$ ; (l) for **16a**; 1-(5-chloro-2-butoxyphenyl)methanamine, same conditions, for **16b**.

Proline-based macrocyclic inhibitors **7–10** were evaluated for their thrombin (IIa), trypsin and tPA inhibitory potencies and their ability to double the activated partial thromboplastin time ( $2\times\text{APTT}$ ) in human plasma.<sup>12</sup> As illustrated in Table 1, we found that *N*-acetyl-4-aminobutyric acid provided the optimal tether between the P<sub>3</sub> amino group and the P<sub>1</sub> phenoxy group (**9**, thrombin  $K_i = 0.4\text{ nM}$ ). Crystallographic analysis of **8** complexed to thrombin (Fig. 2) confirmed the same general binding mode as observed for **2**.<sup>5</sup> The macrocyclic tether is located on the S<sub>4</sub> shelf. Intrinsic potency against trypsin and tPA and selectivity versus thrombin were deemed acceptable ( $>2000$ -fold). While there seemed to be a clear relationship between tether length and inhibitory potency against thrombin, potency was not significantly improved by converting acyclic inhibitor **2** to macrocycle **9**. A more elaborate optimization study was undertaken within the pyrazinone series.

Table 2 documents an extensive study of pyrazinone-based macrocycles. Aliphatic linkers between the P<sub>3</sub> amino group and the P<sub>1</sub> phenoxy group were first evaluated (**17–22**). As observed in the proline series, the inhibitory potency of the compounds is directly related to tether length. A pentyl-derived tether appeared optimal, leading to compound **20**, a  $50\text{ pM}$  thrombin inhibitor, which represents a 40-fold boost in potency when compared to acyclic inhibitors **16a,b** (thrombin  $K_i$ :  $2\text{ nM}$  and  $2.2\text{ nM}$ , respectively). Methylation of the P<sub>3</sub> amino group ( $\text{R} = \text{Me}$ ) provided an additional 2-fold increase in potency resulting in the identification of one of the most potent thrombin inhibitors in this series (**22**, thrombin  $K_i = 20\text{ pM}$ ). The functional activity assay ( $2\text{ APTT}$ ) is, however, a better indicator of potential antithrombotic activity as it reflects both inherent enzyme inhibitory potency and the impact of inhibitor lipophilicity presumably via plasma protein binding.<sup>13</sup> Butyl derivative **19**, when compared to its pentyl analogue **20**, demonstrates that an improvement in thrombin  $K_i$  does not necessarily translate into enhanced functional activity, and that a better balance between potency and physical properties must be achieved. In addition, the selectivity of this set of compounds for inhibition of thrombin over trypsin and tPA was insufficient. While relative selectivity appeared acceptable ( $>100$ -fold), micromolar or higher potencies against serine proteases other than thrombin would be more desirable to avoid potential side effects in a clinical setting. With these two goals in mind, polar functionality was introduced into the macrocycle tether.

Replacement of the tether central methylene with oxygen (**23**) had little effect on intrinsic potency but improved functional activity ( $2\times\text{APTT} = 0.56\text{ }\mu\text{M}$ ), presumably as a result of increased polarity<sup>14</sup> (**23** vs **20**). Selectivity was also improved, especially against tPA. Carbamate derivatives **24** and **25** followed a similar trend with the exception of the saturated derivative **26**.

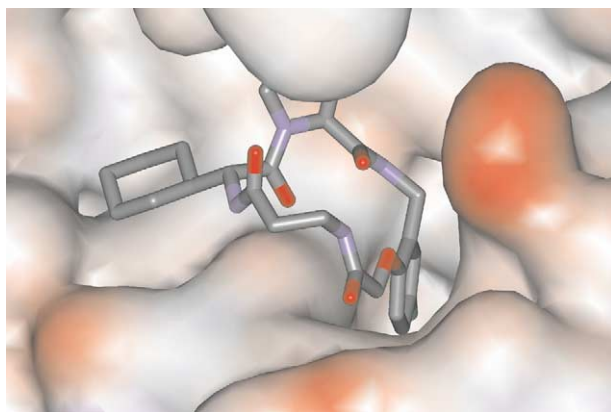
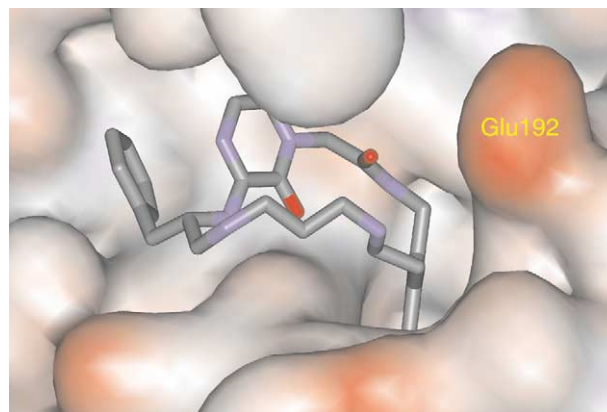
In order to further optimize functional activity and selectivity we then considered the removal of the lipophilic P<sub>1</sub> chloro substituent ( $\text{Y} = \text{H}$  vs  $\text{Cl}$ ). As expected,

**Table 1.** Proline based macrocycles

Compd	<i>n</i>	Thrombin $K_i$ (nM) <sup>a</sup>	2×APTT (μM) <sup>a,b</sup>	Trypsin $K_i$ (μM) <sup>a</sup>	tPA $K_i$ (μM) <sup>a</sup>
<b>7</b>	0	2.9	0.69	9.3	7.7
<b>8</b>	1	1.3	0.36	21.5	5.6
<b>9</b>	2	0.4	0.31	5	8.9
<b>10</b>	3	1.3	0.36	48	4.3

<sup>a</sup> $K_i$  values are the average of at least two determination, standard error of the mean < 10%.<sup>b</sup>The 2×APTT value is the concentration of inhibitor in plasma required to double the activated partial thromboplastin time.**Table 2.** Pyrazinone-based macrocycles of general structure **15**

Compd	X <sub>1</sub>	Y	R	Thrombin $K_i$ (nM) <sup>a</sup>	2×APTT (μM) <sup>a,b</sup>	Trypsin $K_i$ (μM) <sup>a</sup> (selectivity) <sup>c</sup>	tPA $K_i$ (μM) <sup>a</sup> (selectivity) <sup>c</sup>
<b>17</b>	(CH <sub>2</sub> ) <sub>2</sub> -O	Cl	H	560	ND	ND	ND
<b>18</b>	(CH <sub>2</sub> ) <sub>3</sub> -O	Cl	H	26	ND	ND	ND
<b>19</b>	(CH <sub>2</sub> ) <sub>4</sub> -O	Cl	H	0.2	0.74	0.09 (450)	0.02 (100)
<b>20</b>	(CH <sub>2</sub> ) <sub>5</sub> -O	Cl	H	0.05	1.22	0.08 (1600)	0.006 (120)
<b>21</b>	(CH <sub>2</sub> ) <sub>6</sub> -O	Cl	H	0.13	3.17	0.24 (1850)	ND
<b>22</b>	(CH <sub>2</sub> ) <sub>5</sub> -O	Cl	Me	0.02	1.89	0.04 (1800)	0.003 (150)
<b>23</b>	(CH <sub>2</sub> ) <sub>2</sub> -O-(CH <sub>2</sub> ) <sub>2</sub> -O	Cl	H	0.05	0.56	0.11 (2200)	0.15 (3000)
<b>24</b>	CO <sub>2</sub> CH <sub>2</sub> CH=CHCH <sub>2</sub> -O ( <i>Z</i> )	Cl	H	0.06	0.78	0.11 (1850)	0.006 (100)
<b>25</b>	CO <sub>2</sub> CH <sub>2</sub> CH=CHCH <sub>2</sub> -O ( <i>E</i> )	Cl	H	0.17	0.87	0.58 (3400)	0.48 (2800)
<b>26</b>	CO <sub>2</sub> (CH <sub>2</sub> ) <sub>4</sub> -O	Cl	H	0.63	1.97	4 (6300)	ND
<b>27</b>	(CH <sub>2</sub> ) <sub>5</sub> -O	H	H	2.5	0.6	6.7 (2700)	0.36 (150)
<b>28</b>	(CH <sub>2</sub> ) <sub>2</sub> -O-(CH <sub>2</sub> ) <sub>2</sub> -O	H	H	2.1	0.39	4.6 (2200)	3.2 (1500)
<b>29</b>	COCH <sub>2</sub> -NMe-(CH <sub>2</sub> ) <sub>2</sub> -O	H	H	3	0.5	17 (5700)	3.9 (1300)
<b>30</b>	(CH <sub>2</sub> ) <sub>4</sub> -NH-CH <sub>2</sub>	H	H	0.51	0.43	41 (82000)	165 (323000)
<b>31</b>	(CH <sub>2</sub> ) <sub>3</sub> -NH-(CH <sub>2</sub> ) <sub>2</sub>	H	H	0.09	0.47	2.1 (23000)	0.64 (7100)

<sup>a</sup> $K_i$  values are the average of at least two determination, standard error of the mean < 10%.<sup>b</sup>The 2×APTT value is the concentration of inhibitor in plasma required to double the activated partial thromboplastin time.<sup>c</sup>The selectivity value represents the approximate ratio of the trypsin/tPA  $K_i$  to the thrombin  $K_i$ .**Figure 2.** X-ray structure of proline derived macrocycle **8** bound in the active site of thrombin.**Figure 3.** X-ray structure of **31** bound in the active site of thrombin. Residue Glu192 is labelled.

ted,<sup>5a, 15</sup> this resulted in a ca. 50 fold loss in potency (**27** vs **20**) but with an improvement in functional activity. Similarly, removal of the P<sub>1</sub> chloro group from **23** further improved functional activity and selectivity leading to macrocycle **28** with a 0.39 μM 2×APTT value and micromolar potencies against trypsin and tPA. Other modifications of the tether proved fruitful as well. Incorporation of sarcosine into the tether provided inhibitor **29** with a similar profile to **28**. In the light of the previous result, introduction of amino functionality in the linker was studied more extensively. Substitution of one of the tether methylenes with an amino group led to the identification of inhibitors **30** and **31** with acceptable 2×APTT values and exquisite selectivity. In an effort to understand the nature of this newly acquired

selectivity, we turned to X-ray crystallography and molecular modeling.

The crystal structure of the thrombin-**31** complex was determined at 1.8-Å resolution. Glu192, a flexible surface residue located at the top of the S<sub>1</sub> pocket, is not completely resolved in the crystal structure due to its high mobility. The most probable conformation of the side chain, that occupying the region of highest experimental density, is shown in Figure 3. In the crystal structure, no direct salt bridge is observed, but a solvent-separated salt bridge between the amino group of the linker and glutamate side chain remains possible. A rotamer of the Glu192 side chain generated using molecular modeling techniques does allow for a direct

interaction between the phenethylamine nitrogen of **31** and the side chain and may contribute to the inhibitor's potency.

In the case of the benzylamino analogue **30**, on the other hand, both direct and water-mediated salt bridges with Glu192 are precluded by the linker. In the modeled complex,<sup>16</sup> the protonated amine participates in inter- and intramolecular hydrogen bonds, to Gly216 and the P<sub>1</sub>-P<sub>2</sub> linker carbonyl respectively. These hydrogen bonds, along with the overall negative charge of this region of the active site caused by the proximity of Glu192, offset the energy of desolvating the highly polar protonated amine and result in a modest loss of potency relative to **31**. In contrast, the analogous residue to thrombin's Glu192 in both tPA and trypsin is Gln192. As a result, whereas thrombin carries a net negative electrostatic potential in this region of the active site, this region is nearly electroneutral in trypsin and carries a slight positive potential in tPA due to the presence of nearby basic residue Lys143. The change in electrostatic potential helps rationalize the poor potency of **30** for trypsin and tPA, which unlike thrombin cannot offset desolvation of the amino group with favorable electrostatic interactions.<sup>17</sup>

In conclusion, we have described the design, preparation, and evaluation of a series of macrocyclic proline and pyrazinone thrombin inhibitors. In the case of pyrazinone derivatives, macrocyclization resulted in significant improvements in potency relative to acyclic analogues. The SAR observed led us to incorporate specific functional groups in the tether resulting in enhanced functional activity against thrombin and exquisite selectivity against trypsin and tPA. Crystallographic and molecular modeling studies revealed the interactions between inhibitors and residue Glu192 which allow for such high selectivity.

### Acknowledgements

We thank M. Bogusky, J. Murphy, S. Pitzenberger, S. Varga, A. Coddington, C. Ross, H. Ramjit, K. Anderson, P. Ciecko and M. Zrada for analytical support, and Kristen Glass for technical assistance in the preparation of **10**.

### References and Notes

1. *Thrombosis in Cardiovascular Disorders*; Fuster, V., Verstraete, M., Eds.; W.B. Saunders: Philadelphia, 1992.
2. Parenteral administration of low molecular weight heparin and intense patient monitoring required with warfarin limit their chronic utility.
3. Adang, A. E. P.; Rewinkel, J. B. M. *Drugs Future* **2000**, 25, 369.
4. Coburn, C. A. *Exp. Opin. Ther. Patents* **2001**, 11, 1. Sanderson, P. E. J. *Annu. Rep. Med. Chem.* **2001**, 36, 79. Vacca, J. P. *Annu. Rep. Med. Chem.* **1998**, 33, 81.
5. (a) Tucker, T. J.; Brady, S. F.; Lumma, W. C.; Lewis, S. D.; Gardell, S. J.; Naylor-Olsen, A. M.; Yan, Y.; Sisko, J. T.; Stauffer, K. J.; Lucas, B. J.; Lynch, J. J.; Cook, J. J.; Stranieri, M. T.; Holahan, M.; Lyle, E. A.; Baskin, E. P.; Chen, I. W.; Dancheck, K. B.; Krueger, J. A.; Cooper, C. M.; Vacca, J. P. *J. Med. Chem.* **1998**, 41, 3210. (b) Tucker, T. J.; Lumma, W. C.; Mulichak, A. M.; Chen, Z.; Naylor-Olsen, A. M.; Lewis, S. D.; Lucas, B. J.; Freidinger, R. M.; Kuo, L. C. *J. Med. Chem.* **1997**, 40, 830.
6. Burgey, C. S.; Robinson, K. A.; Lyle, T. A.; Sanderson, P. E. J.; Lewis, S. D.; Lucas, B. J.; Krueger, J. A.; Lyle, E. A.; Stranieri, M. T.; Holahan, M.; Sitko, G. R.; Cook, J. J.; Wallace, A. A.; Clayton, F.; Bohn, D.; Leonard, Y.; Detwiler, T.; Lynch, J. J.; Williams, P. D.; Coburn, C. A.; Dorsey, B. D.; McMasters, D. R.; McDonough, C. M.; Sanders, W. M.; Gardell, S. J.; Shafer, J. A.; Vacca, J. P. *J. Med. Chem.* **2003**, 46, 461.
7. For simplicity we will refer to that end of the inhibitor which binds to the distal hydrophobic binding pocket as P<sub>3</sub>. The region of the enzyme active site overlying Gly216, Glu217, and Gly219, which bridges the distal hydrophobic pocket and the S1 specificity pocket, we will refer to as the S<sub>4</sub> shelf to distinguish it from the distal hydrophobic binding pocket. Inhibitor moieties occupying this region of the active site we will call P<sub>4</sub>.
8. (a) Tyndall, J. D. A.; Fairlie, D. P. *Curr. Med. Chem.* **2001**, 8, 893. (b) Greco, M. N.; Maryanoff, B. E. *Adv. Amino Acid Mimet. Peptidomimet.* **1997**, 1, 41. (c) Greco, M. N.; Powell, E. T.; Hecker, L. R.; Andrade-Gordon, P.; Kauffman, J. A.; Lewis, J. M.; Ganesh, V.; Tulinsky, A.; Maryanoff, B. E. *Bioorg. Med. Chem. Lett.* **1996**, 6, 2947. (d) Maryanoff, B. E.; Zhang, H. C.; Greco, M. N.; Glover, K. A.; Kauffman, J. A.; Andrade-Gordon, P. *Bioorg. Med. Chem.* **1995**, 3, 1025.
9. Horwell, D. C.; Hugues, J.; Hunter, J. C.; Pritchard, M. C.; Richardson, R. S.; Roberts, E.; Woodruff, G. N. *J. Med. Chem.* **1991**, 34, 404.
10. Nantermet, P. G.; Selnick, H. G. *Tetrahedron Lett.* **2003**, 44, 2401.
11. Furstner, A.; Langemann, K. *Synthesis* **1997**, 792.
12. Lewis, S. D.; Ng, A. S.; Lyle, E. A.; Mellott, M. J.; Appelby, S. D.; Brady, S. F.; Stauffer, K. S.; Sisko, J. T.; Mao, S.-S.; Veber, D. F.; Nutt, R. F.; Lynch, J. J.; Cook, J. J.; Gardell, S. J.; Shafer, J. A. *Thromb. Haemost.* **1995**, 74, 1107.
13. Tucker, T. J.; Lumma, W. C.; Lewis, S. D.; Gardell, S. J.; Lucas, B. J.; Baskin, E. P.; Woltmann, R.; Lynch, J. J.; Lyle, E. A.; Appleby, S. D.; Chen, I.-W.; Dancheck, K. B.; Vacca, J. P. *J. Med. Chem.* **1997**, 40, 1565.
14. Calculated LogP (ChemDraw) for **20** and **23** are 3.7 and 2.6, respectively.
15. Lumma, W. C.; Witherup, K. M.; Tucker, T. J.; Brady, S. F.; Sisko, J. T.; Naylor-Olsen, A. M.; Lewis, S. D.; Lucas, B. J.; Vacca, J. P. *J. Med. Chem.* **1998**, 41, 1011.
16. (a) Multiple conformations of the macrocycles were generated using the metric matrix distance geometry algorithm JG (S. Kearsley, Merck & Co., Inc., unpublished). The generated conformers were energy-minimized within the thrombin active site using MacroModel (ref 17b) with the MMFF force field, and allowing Glu192 to adjust to the inhibitor. (b) Mohamadi, F.; Richards, N. G. J.; Guida, W. C.; Liskamp, R.; Lipton, M.; Caufield, C.; Chang, G.; Hendrickson, T.; Still, W. C. *J. Comput. Chem.* **1990**, 11, 440.
17. Differences in electrostatic potential caused by E/Q192 have been proposed as an important factor in the selective binding of PAI-1 to tPA versus thrombin. Rezaie, A. R. *Biochemistry* **1998**, 37, 13138.